AN ANALYSIS OF X-RAY DATA OBTAINED FROM
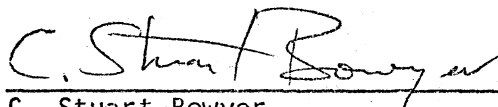
THE SOURCE SCO XR-1

A THESIS

SUBMITTED TO THE NATIONAL COUNCIL

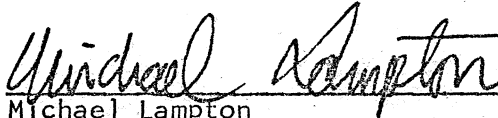OF SPACE ACTIVITIES (CNAE) OF BRAZIL

by

Walter González Alarcón

IN PARTIAL FULFILLMENT OF THE REQUIREMENTS

FOR THE DEGREE OF MASTER OF SCIENCE

APPROVED:

C. Stuart Bowyer
Professor of Astronomy
University of California, Berkeley

Michael Lampton
Instructor of Physics (Acting)
University of California, Berkeley

DECEMBER, 1969

To My Parents

ACKNOWLEDGMENTS

I am most grateful to the National Council of Space Activities (CNAE) of Brazil for the opportunity given to me in doing this work.

I would like to express my deepest appreciation to Dr. Stuart Bowyer, Dr. Michael Lampton, and Mr. John Mack for their invaluable guidance and suggestions about many topics of the thesis.

Lastly, I would like to mention my gratitude to Miss Helen Schwartz and Mrs. Robin Zoesch for their help in typing the manuscript.

ABSTRACT

On June 22 of 1969 an Aerobee rocket was launched in
Natal, Brazil, as a cooperative program between the National
Council of Space Activities of Brazil (CNAE) and the Space
Sciences Laboratory of the University of California, Berkeley.

The objective was to search for new galactic X-ray
sources, to detect some of the known ones, and to study the
interplanetary medium as an absorbing region for X-rays.

In this work we present the analysis of the galactic
source SCO XR-1 which has been detected during the experiment.

We have found that the best model for SCO XR-1 is
Thermal Bremsstrahlung from a Hot Plasma with a temperature
corresponding to 9.8 Kev and a column density of absorbing
atoms of 1.8×10^{21} atoms/cm^2. The measured energy range
goes from 0.1 Kev to 10.0 Kev.

Index

1. INTRODUCTION

One of the first totally unexpected results of space astronomy was the discovery of strong X-ray sources outside the solar system. The energy of the range of the emitted radiation is about 0.1 to 100 Kev (nearly 124 to 0.124 A).

The discovery of cosmic X-ray sources was preceded by more than a decade of observations of X-ray emission from the Sun. In the course of such observations in 1956, evidence of the existance of an istropic X-ray background flux was obtained by Kupperian and Friedman[1]. Subsequent observations[2] set upper limits on fluxes from any discrete cosmic X-ray sources at a level of about 10^{-8} erg/cm^2/sec in the 1 to 10 Å range. No instruments capable of exceeding this limit of detection were flown, however, until June of 1962 when Giacconi, Gursky, Paolini and Rossi of M.I.T.[3] employed Geiger counters which were an order of magnitude more sensitive than those flown previously. The improved instrumentation detected a source of X-rays displaced from the direction of the Moon, which was the primary target of observation. No collimation has been provided to define the source direction precisely. The results revealed the existence of a strong source in the constellation Scorpius not far from the galactic center and a diffuse X-ray background, apparently also of celestial origin.

At the present time, more than 40 discrete sources have been detected. All but a few lie close to the galactic plane and, undoubtedly are galactic objects. Estimates of the X-ray sources luminosities (0.1-100 Kev) are of the order of 10^{36} erg/sec, 1000 times the visible luminosity of the Sun and more than 10^{12} times the X-ray luminosity of the quiet Sun in the same energy band. In galactic sources in which optical and radio counterparts have been found, the X-ray luminosities are one to two orders of magnitude greater than

the optical and radio luminosities.

Since the Earth's atmosphere absorbs these X-rays very strongly, measurements must be made from sounding rockets or satellites, or at least the instruments must be carried to balloon altitudes from which a limited class of experiments can be performed. In addition to the limitations in weight and volume imposed by the experiment carrier, one no longer has the very rigid inertial platform provided by the Earth. The experimenter must provide the means for stablizing the carrier and determining its orientation with respect to the celestial sphere. Also, the very low fluxes of radiation make the use of efficient quantum detectors mandatory. The ultimate limit in precision and sensitivity is invariably the statistical fluctuations in the number of recorded photons. Finally, X-ray focusing optics with their potential for high-resolution imagery and the various techniques for high-dispersion spectroscopy have not yet been utilized in celestial studies. Angular resolution has been achieved with mechanical collimators, and spectra have been measured by nondispersive techniques.

No generally accepted models exist for any of the X-ray sources, which is, in part, a reflection of the relative crudeness of the X-ray measurements. The two physical mechanism that seem to be capable of providing the X-ray emissions are the Synchrotron radiation from ultrarelativistic electrons gyrating in a magnetic field and the thermal emissions from an extremely hot plasma. These and other possibilities are subject to experimental verification.

On June 22 of 1969 an Aerobee rocket was launched in Natal, Brazil, as a cooperation program between the National Council of Space Activities of Brazil (CNAE) and the Space Sciences Laboratory of the University of California, Berkeley. The rocket carried proportional counters with honeycomb collimators. It was a freely spinning rocket and scanned SCO XR-1 at an average altitude of 108 Km.

We have developed a suitable program for fitting the data to different possible source models. Using this program together with the measured data of this experiment we present in this work a spectrum analysis for SCO XR-1. The models used are Bremsstrahlung from a hot plasma, Black Body radiation, Synchrotron mechanism and Inverse Compton scattering. The last two processes result in a Power Law spectrum. We used the X^2 Test for choosing the suitable parameters which for each model describe the associated process. For each case we include the effect of interstellar absorption.

It has been found that the best fit is obtained for Thermal Bremsstrahlung from a Hot Plasma with a temperature of 11.4 x 10^7 °K (9.8 Kev) and with a line of sight absorption of 1.8×10^{21} atoms/cm^2. This may be the effect of self-absorption in the source or the interstellar medium.

2. X-RAY DETECTORS

A necessary requirement of detectors for X-ray astronomy is high efficiency and large effective area because the flux at X-rays show celestial sources is quite small as measured at the earth. A variety of detectors have been used for cosmic X-ray measurements, but the most common up-to-date is the proportional counter for X-rays with energies between 1 and 10 Kev.

2.1 Proportional Counter

This detector is fabricated so that a high electric field gradient is obtained near the positive electrode. The cathode usually also serves as the gas container and main structural member, and contains a thin entrance window for the X-rays.

An X-ray photon that is absorbed in the counter gas usually ionizes an atom of the gas by ejecting a phtoelectron from the tightest bound level allowed by energy conservation. The photoelectron will interact with the gas and result in additional electron-ion pairs; eventually its energy will be dissipated and a cloud of electronic pairs will remain along its path. The original ion usually will de-excite by emitting Auger electrons, although it may emit its characteristic line radiation (fluorescence yield). The Auger electrons also will interact with the gas and result in electron-ion pairs. If no fluorescence photons escape the counter, the total number of electron-ion pairs is proportional to the incident photon energy within the bounds of statistical fluctuations.

The initial electron cloud then drifts toward the anode because of the electric field in the counter. When the electrons enter the high electric field region near the anode they receive sufficient energy between collisions so that further ionization of the gas occurs, the secondary electrons create additional secondary electrons, and the number of electrons continues to increase until they are collected by the anode. Gas gains of 10^3 to 10^5 are readily achieved in this manner.

A noble gas is usually chosen for the primary counter-gas constituent

because of the higher obtainable gas gain and initial ionization; this is a consequence of the fact that nonionizing energy loss mechanisms, such as excitation of low-level rotation or vibration states in a polyatomic molecule, are absent or less probable in the noble gas. A polyatomic quench gas, such as methane, carbon dioxide, or alcohol, is usually added to the counter to absorb the ultraviolet light from the noble gas and allow the noble-gas atoms in metastable states to de-excite by collisions with the quench-gas molecules. The mean free path for these events is small and the electrons ejected from the quench gas are ejected near the anode at the time and place of the gas multiplication occuring during the original pulse and therefore do not start a secondary avalanche at a later time.

The intrinsic efficiency of the counter is the probability of the photon not being absorbed in the window and then being absorbed in the gas. Since the photoelectric cross section varies approximately as $(Z^4/E^{8/3})$ in the few-Kev region, it is important to have a thin, low-Z window and a thick, high-Z gas. Beryllium and metallized Mylar have found widest application as window materials. For soft X-rays (from 0.1 to 10 Kev.) and low to moderate-Z materials, we can neglect scattering compared to absorption and the efficiency is approximately: $\mathcal{E}(E)=\exp(-\mu_w X_w)[1-\exp(-\mu_g X_g)]$ ....1 where $\mathcal{E}$ is the counter efficiency, X_w and X_g are the window and gas thickness, μ_w and μ_g are the absorption coefficients of the window and the gas at the energy E. The efficiency calculated for the counter used in the experiment is shown in figure 1. The absorption edges and the effect of window thickness on the efficiency at low energy is particularly noticeable. The charge collected at the anode is proportional to the number of initial electrons and the gas gain of the counter, and can be used to measure the photon energy. The spectral resolution primarily depends upon the fluctuations in the number of initial electrons and the gas gain.

The energy resolution may be degraded by gain dependence on the location of the event in the counter. This may be caused by nonuniform fields near the ends of the counter and variations in anode finish and thickness. Some authors[4] have performed an extensive energy resolution study and found that, under optimum conditions, the fractional energy resolution of 0.1 Kev $< E < 10$ Kev can be expressed as 0.14 $E^{-1/2}$; where E is in Kev. The time resolution of the proportional counter is necessary for planning coincidence or anticoincidence requirements. Since the initial photoabsorptions can occur anywhere in the counter, the time resolution corresponds to the drift time of an electrode from the cathode to the anode. For a counter with a 2-inch square cathode and a 0.002-inch diameter anode operated at 2200V this time was found to be $0.8 \mu sec$ for a 90 percent argon, 10 percent CH_4 gas filling[5].

2.2 Geiger Counter

The early experiments[3,6] in X-ray astronomy were conducted with thin-window Geiger Counters. The Geiger counter is similar to a proportional counter but is operated at such a high gas gain that the characteristics of the pulse depend on the saturation characteristics of the counter and associated circuiting rather than expose the initial event. A large standard pulse that simplifies electronic requirements is obtained, but the energy informative is lost and the recovery time is increased. The effective background will include events that would fall outside the selected X-ray energy region in the proportional counter.

2.3 Photoelectric Detector

Gas counters cannot be operated in a vacuum without a window and each window places a low-energy limit to the observable position of the X-ray spectrum. The photoelectric detector does not need a window and can therefore, be used to extend the measurements to lower photon energies than are accessible to gas counters.

The possibility of building a photoelectric detector for X-rays was discussed by a group of Russian Scientists in 1960[7] and rests on the fact that several alkali halides have an anomalously high photoelectric yield for X-rays. The photocathode is an evaporated layer of KCl or CsI deposited on a spherical surface.

2.4 Scintillation Detector

Na(Tl) scintillation counters were first used in 1964 by Clark to observe X-rays from the Crab Nebula from a balloon[8], and by Giacconi, Gersky and Walters[9] to observe X-ray from SCO XR-1 from a sounding rocket. Scintillation counters were utilized well before this time to measure high-energy solar X-rays by Chubb, Friedman and Kreplin[10].

The device, discussed extensively in the literature[11], consists of a scintillating crystal and phototube. The scintillator must include some moderate-to high Z components to be efficient at the upper end of the effective energy range and also so that the photoelectric effect will be the dominant energy-absorption mechanism. The latter property is necessary for optimum energy resolutions since the competing process, Compton scattering, does not result in a unique energy deposition in the scintillator.

2.5 X-ray Telescope

The fact that X-rays will reflect with high efficiency at grazing incidence allows the construction of optical systems for X-rays. The first proposal for using X-ray optical systems for astronomical observations was made by Giacconi and Rossi[12] who suggested various kinds of collectors for concentrating the X-rays entering a large-aperature device into a small focal spot. Giacconi's group constructed the first paraboloid hyperboloid combination of grazing surfaces for producing astronomical images; this instrument was first used in a joint experiment with Goddard Space Flight Center to obtain photographs of the Sun in X-rays[13].

Focusing telescopes will clearly be important in studying non-solar X-ray sources, since they allow measurements qualitatively different from those which can be accomplished with conventional mechanical collimators. Because of the high intrinsic spatial resolution, source structure can be studied in detail and celestial position can be precisely established. Focusing devices also allow the use of certain dispersive techniques to obtain high spectral resolution.

2.6 Collimators

2.6.1 Cellular Collimator

In order to obtain accurate information on the location of the X-ray sources and on their angular sizes, it is necessary to limit the field of view of the detectors by means of suitable collimators. Because of the large area of the detectors and of the limited space available, cellular type collimators have been used. With those collimators one can obtain fields of view of different shapes and different angular widths down to about two degrees. The transmission is a maximum for a beam parallel to the axis fo the collimator. The response curves have typically nearly triangular shapes. One type of this collimator is that known as "Honeycomb collimator."

2.6.2 Modulation Collimator

In order to improve the angular resolution of a cellular collimator, it is necessary to decrease its field of view. In this manner, however, one also decreases the number of counts recorded when the X-ray source passes across the field of view, and therefore, one reduces the statistical accuracy of the data. There is thus a practical limit to the resolution that may be obtained with these devices when used on spinning rockets.

A collimator of a different type, which combines high resolution with wide field of view was conceived by M. Oda [14] and has been developed by the ASE-MIT group. Known as the "modulation collimator", it consists essentially of a series of plane grids of parallel wires placed one in

front of the other at a suitable distance. The diameter of the wires

is nearly equal to the spacing between adjacent wires. In a parallel

beam of rays, the front grid casts a shadow on the rear grid. The

shadow shifts as the orientation of the collimator relative to that

of the incident beam changes, and the transmission of the collimator

changes correspondingly, being a maximum when the shadow of the front

wires falls exactly on the back wires, and a minimum when it is cen-

tered between adjacent wires. With this collimator one can obtain

fields of view as small as a few arc seconds.

3. THEORETICAL MODELS

We now have reviewed the fundamental X-ray generation mechanisms which are considered likely for localized stellar sources of X-rays. Generation of X-rays is contingent upon the acceleration of charged particles, and in this case only electrons are important. Since the radiated power P by an accelerated charged particle goes as:

$$P = 2/3 \frac{e^2}{c} (\dot{\vec{\beta}})^2 \qquad ; \qquad \beta = \frac{v}{c} \ll 1$$

and

$$P = 2/3 \frac{e^2}{c} \gamma^6 \left[(\dot{\vec{\beta}})^2 - (\vec{\beta} \times \dot{\vec{\beta}})^2 \right] \quad \cdots \cdots \quad 2$$

for relativistic velocities (15), where $\gamma \equiv \frac{1}{(1-\beta^2)^{1/2}}$, the power radiated is proportional to the square of the acceleration $\dot{\vec{\beta}}$. The electromagnetic forces on electrons and other charged particles are only dependent upon charge and velocity; however, the much smaller rest mass of the electron results in acceleration $\sim$ 2000 times that of protons, for equal electromagnetic forces. Assuming electrons and protons of equal Kinetic energy, γ for electrons is ~2000 times that for protons. The dependence on γ in equation 2 above, further enhances the electron contribution for relativistic energies. In the first case below, we consider acceleration of an electron due to a magnetic field, either a field of spatial extent (synchrotron radiation) or that due to the electromagnetic field of a colliding photon (inverse Compton radiation). The second case considers the radiation produced due to acceleration of the electron in the field of an atomic nucleus. A third case considered is that of "black body" radiation, which is the thermal radiation emitted by a body when the body is optically thick for photons of the energy considered.

3.1 Power Law Models

3.1.1 Synchrotron Radiation

This kind of radiation caused by the acceleration of electrons in a magnetic field is thought to be responsible for much of the emission observed from celestial point sources in the radio range. First observed in synchrotrons, the radiation is characterized by a high degree of polarization since the direction of the electron acceleration is always perpendicular to its velocity and to the magnetic field B. Thus the radiation viewed perpendicular to B is linearly polarized (electric field vector perpendicular to the existing B field). Viewed parallel to B, the radiation is circularly polarized and it is thus elliptically polarized between these two extremes. For $V/C \ll 1$, the emission is at ν_c, the cyclotron frequency:

$$\nu_c = \frac{e B \perp}{2 \pi m c}$$

where m is the rest mass of the electron, while for $V/C \sim 1$, the emission pattern becomes very pronounced in the forward direction, and higher harmonics are introduced. Schwinger[16] has investigated this theoretically, and Corson[17] and others have verified the results on synchrotrons. The average power emitted per unit frequency for an electron of total energy E is found to be

where

$$\bar{P}(\nu) = \frac{\sqrt{3}}{\pi^2} \left(\frac{e^2}{m c^2} \right) \frac{E}{R} F\left(\frac{\nu}{\nu_m} \right) \quad \ldots \ldots \ldots \ldots \quad 3$$

$$\nu_m = 3/2 \left(E / m c^2 \right)^2 \nu_c \quad \ldots \ldots \ldots \ldots \ldots \quad 4$$

$R = \frac{m V c \gamma}{e B}$ is the instantaneous radius of the orbit, and $F\left(\nu/\nu_m \right)$ is a

slowly varying function. The maximum emission per frequency interval

occurs near $\nu = \nu_m/5$, with the half power points near $10^{-2} \nu_m$,

and ν_m . Schwinger shows that for a circular orbit,

$$P_n = \frac{4(3^{1/6}) \; \Gamma(2/3) \, e^2 \, \nu_c^2}{\beta \, c} \left(m c^2/E\right) n^{1/3} \quad ; \quad \nu \ll \nu_m \; \ldots \ldots \; 5$$

while for $\nu \gg \nu_m$ the spectrum decreases exponentially:

$$P_n = \frac{3^{3/2} \, \pi^{3/2} \, e^2 \, \nu_c^2 \, n^{1/2} \, e^{-n/n_m}}{2^{1/2} \, \beta \, c \, n_m^{3/2}}$$

where P_n is the power radiated per unit frequency in the nth haromonic

of ν_c , and Γ is the gamma function. The total power radiated is

given by

$$\bar{P}(E) = 2/3 \; \frac{e^2 \, \nu_c^2}{4 \, c \, \pi^2} \left[\left(E/m c^2\right)^2 - 1 \right] \quad \ldots \ldots \ldots \; 6$$

Although synchrotron radiation is believed important at radio frequencies,

the mechanism requires rather high energy electrons for emission of X-rays.

For example, in a 10 microgaus field, for $h\nu_m = 1$ Kev, electron energies

of $\sim 10^{10}$ Kev are required. If one assumes a power law spectrum of

electrons (e.g., cosmic rays), $dN/dE = AE^{-K}$, and assumes that all the

synchrotron radiation for an electron of energy E occurs at $\nu = \nu_m$

then the X-ray number spectrum is also a power law:

$$dN/dE = A_1 \, E^{-(K+1)/2} \quad \ldots \ldots \ldots \ldots \; 7$$

Thus a power law is expected for X-rays if the generating electron spec-

trum is a power law.

3.1.2 Inverse Compton Radiation

An electron will also radiate due to interaction with an electro-

magnetic field, such as that due to a starlight photon. If the electron

is relativistic, and the photon of energy $h\nu \ll m_e c^2$, the interaction

is often called an "inverse" Compton process. Although in this case the

electron transfers energy to the photon, instead of vice versa, the interaction can be treated simply as a Compton scattering process merely by a transformation to the rest system of the electron. (This is indicated by the symbol "'".) The photon energy in this system is then given by the expression:

$$(h\nu)'_i = \gamma \, (h\nu)_i \, (1 + \beta)$$

for a head-on collision, where h is the Planck constant, ν is the photon frequency, and γ, β refer to the velocity of the electron in the "Lab" system. The subindex i means "before the collision." After the collision, the photon energy is given by the expression:

$$(h\nu)'_f = (h\nu)'_i \, / \, 1 + \alpha \, (1 - \cos \theta') \qquad ; \quad \alpha = (h\nu)'_i \, / mc^2$$

where mc^2 is the rest mass of the electron and $\cos \theta'$ is the scattering angle. The subindex f means "after the collision." If we suppose $\gamma > 10^3$, then $\alpha \ll 1$ and $(h\nu)'_f \sim (h\nu)'_i$ with merely a reverse in the momentum direction for a head-on collision. Then the final energy of the photon in the "Lab" system is given by:

$$(h\nu)''_f = \gamma \, (h\nu)'_f \, (1 + \beta) \sim \gamma^2 \, (h\nu)_i \, (1 + \beta)^2$$

for a head-on collision, where the sign in the parenthesis is again positive because of the change in the direction of the photon momentum in the rest system of the electron. We thus see that the final energy is approximately γ^2 times the initial energy, which is analogous to the energy dependence discussed earlier for synchrotron radiation (equation 4) VIZ:

$$\nu_m = (3 \, / \, 2)(E \, / \, mc^2)^2 \, \nu_{cf} \sim \gamma^2 \, \nu_{ci}$$

As is the case for synchrotron radiation, inverse Compton scattering gives a distribution of photon energies, since all collision angles are of course possible. As we already pointed out, for both processes we

can approximate the radiated power by the expression:

$$I(E) = A_i E^{-\alpha_i} \quad , \quad \alpha_i = \frac{K+1}{2} \quad \cdots\cdots\cdots \quad 7'$$

where A_i is a normalization factor.

3.2 Thermal Bremsstrahlung from a Hot Plasma

The intensity of radiation from a hot Maxwellian plasma is usually represented by the approximation $I(E) = A_{exp}\left(^{-E}/_{KT}\right)$ where $I(E)$ is the intensity, A is a constant, KT is the temperature of the plasma in electron volts (K is the Boltzmann constant = $.86 \times 10^{-7}$ KeV /°K) and E is the X-ray energy. However, a more exact expression for $I(E)$ can be derived by using the non-relativistic Borne approximation. Using the cross section, the dependence of radiation intensity $I(E)$ on photon energy (E) can be derived. A in detail review article by Koch and Motz (1959) covers these points. It is assumed that the source is isothermal with temperature (KT) of several Kev, and that all the radiant energy is in the continuum. At this temperature, energy in emission lines is expected to be small and structure caused by absorption edges in the X-ray region is also small (Tucker and Gould, 1966) if one assumes the cosmic abundances given by Allen (1958). The calculation is good for emission from a region where the plasma density is small enough so there is no attenuation of the radiation in the source.

Assume a region containing plasma with constant density P, free electrons /cm^2 and total number of electrons Ne. The electrons have a Maxwellian velocity distribution characterized by the non-relativistic temperature KT measure in Kev. The Elwert factor is used to make the high-frequency limit of the cross section correct. It is assumed that there is no screening of the nucleus by atomic electrons.

The radiated intensity is computed by folding this Bremsstrahlung

cross section with the Maxwellian electron energy distribution times

the electron velocity. To calculate I(E), the integral is performed

over all electron energies E. Putting in numbers for the atomic

constants, the radiated intensity is given by:

$$I(E) = \gamma/(KT)^{3/2} \int_E^\infty e^{-E'/KT} \; Ln\left(\frac{\beta + \beta'}{\beta - \beta'}\right) \frac{\beta}{\beta'} \left[\frac{1 - exp(-2\pi Z/137\beta)}{1 - exp(-2\pi Z/137\beta')}\right] dE'$$

where

$$\gamma = 1.68 \times 10^{-15} \left(Z^2 N_e \; \rho \right) \qquad \cdots \cdots \cdots \; 8$$

$$\beta = (2E'/mc^2)^{1/2}$$

$$\beta' = [2(E'-E)/mc^2]^{1/2}$$

The term KT is in units of Kev and I(E) is in Kev/Kev-sec. The term

β/β' times the last term in the integral is the Elwert factor. The

lower limit E of the integral is the photon energy for which the intensity

I(E) is to be computed. Electrons with energies less than E cannot con-

tribute to I(E).

At low frequencies, $E \ll KT$, $\beta = \beta'$, so the Elwert factor is ~ 1 and the

above integral becomes:

$$KT \left[0.81 + Ln(KT/E) \right]$$

The long wavelength limit of the expression for the radiated intensity

is therefore

$$I(E) = \gamma/(KT)^{1/2} Ln(2.25 \; KT/E) \qquad \cdots \cdots \cdots \cdots \; 9$$

For low Z material and all photon energies, the Elwert factor is not

large. If this factor is set equal to unity, expression for I(E) (equation

8) can be integrated (Wharton, 1969) and becomes

$$I(E) = \gamma/(KT)^{1/2} \left[e^{-E/2KT} K_0(E/2KT) \right] \qquad \cdots \cdots \; 10$$

The term K_0 is a modified Bessel function of the second Kind.

For $E \ll KT$; $K_0(E/2KT) = Ln(4KT/E) - 0.577$

$E \gg KT$; $K_0(E/2KT) = (\pi/2)^{1/2} \dfrac{e^{-E/2KT}}{(E/2KT)^{1/2}}$

Thus, the long wavelength limit for $I(E)$ is identical to that given previously.

3.3 Black Body Radiation

When the number density in the plasma becomes so high that the plasma is no longer optically thin for photons of a given energy, the radiation approaches a black body distribution for that energy.

The bremsstrahlung formulae no longer apply and the emission now goes as the surface area of the body and is given by the Planck function:

$$I(E) = 2\pi/h^2 c^2 \; E^2 \left[\exp(-E/KT) - 1 \right] \quad \ldots \ldots \ldots 11$$

The total power radiated is the integral of the above expression:

$$\bar{I} = \sigma T^4, \text{ where } \sigma = 5.67 \times 10^{-5} \; ergs/cm^2 \; sec.deg.^{-4}$$

4. ATMOSPHERIC AND INTERSTELLAR ABSORPTION

Because of atmospheric absorption, X-rays cannot be observed with ground-based instruments. The altitude requirements for X-ray astronomy become clear from our examination of figure 2a, showing the altitude where electromagnetic waves of different wavelengths arrive with different degrees of attenuation. One sees that X-rays with wavelength greater than about one $\overset{o}{A}$ (quantum energy E smaller than 12 Kev) can be observed only at altitudes greater than 50 Km, which can be reached only by rockets or space vehicles. X-rays with quantum energies E greater than about 15 Kev, on the other hand, penetrate to altitudes of the order of 30 Km, which are within the range of balloon flights.

The absorption of X-rays does not end outside the Earth's atmosphere. The interstellar medium is a strong absorber of X-rays; its X-ray absorbing characteristics have been estimated by a number of investigators (18, 19, 20, 21). In figure 2b we show the results of the calculation by Brown and Gould. In the X-ray energy region the absorption takes place predominantly in the higher-Z elements such as oxygen and neon. Since the cosmic abundance of these elements is not known to better than about a factor of two, there is a corresponding uncertainty in the X-ray absorption coefficient.

The absorptive effect of the interstellar medium can be expressed by the relation

$$\phi'(E) = \exp\left[-\tau(E)\right] \phi(E)$$

where $\phi(E)$ is the differential X-ray spectrum in units of number of photons per unit energy interval at an energy E, ϕ' is the observed spectrum, and $\tau(E)$ is the optical depth along the line of sight. Except for the presence of absorption edges, $\tau(E)$ varies approximately as the 8/3 power of the X-ray energy, and is a decreasing function of energy.

Because of this strong energy dependence, and since the absorption enters as an exponential factor, the effect of the interstellar absorption is to produce a relatively sharp cutoff at some low energy.

The quantity $\tau(E)$ is derived from more elementary constants through the following relation:

$$\tau(E) = \ell \sum_i N_i \sigma_i(E)$$

Where ℓ is the distance to the source, N_i is the average number density of the ith element, and $\sigma_i(E)$ is the cross section for X-ray absorption of that element at an energy E. The sum must, of course, extend over all elements; but, as noted, the principal contribution to $\tau(E)$ will originate in only several elements. It is frequently more convenient to quote the number $N_H\ell$, the column density (H atoms/cm^2) of hydrogen atoms to the source, since this quantity is sometimes directly available on the basis of 21-cm radio data. One can specify the energy E_0 at which $\tau(E)$ is unity, in which case $\tau(E)$ can be replaced by $(E_0/E)^{8/3}$. There is some evidence for finite absorption effects in several X-ray sources. In this work we found a turnover at about 3 Kev in the X-ray spectrum of SCO XR-1 and we assume it is due to absorption. Unfortunately, observations of a turnover in the spectrum cannot be unambiguously assigned to the effects of the interstellar medium; the absorbing layer could be intrinsic to the X-ray source itself. Several measurements can yield the X-ray absorption of the interstellar medium more or less unambiguously. One is simply the observation of low-energy cutoffs in sources for which the distance is known and for which there is some basis for specifying the spectrum at the source before the absorption. Another measurement is of the low-energy cutoff of the diffuse X-ray background. If that background is of extra-galactic origin, the cutoff will vary systematically as a function of the galactic latitude.

Bowyer, Field and Mack (6) may have observed this effect.

The presence of interstellar absorption severely limits observations at low energy; at energies below about 0.5 Kev useful measurements can be made on objects only within about 100 pc of the Earth. On the other hand, the galactic disk should be transparent at energies above about 4 Kev, and outside the galactic disk the density of matter is sufficiently low to permit the observation of extragalactic objects to cosmological distances.

In principle at least, the observation of absorption effects can yield the following information:

a) The distance to the source, if there is an independent measurement of $N_H \ell$.

b) The abundance of certain elements in the interstellar medium. The observation of an edge discontinuity gives directly the number of atoms of the elements that contribute to the edge.

c) Information about the nature of the source, if the absorption can be placed at the source rather than within the interstellar medium.

The X-ray absorption measurement is related to a number of other measurements of the properties of the interstellar medium, notably the 21-cm emission in radio, interstellar absorption lines at optical frequencies, and interstellar reddening; and measurements of the absorption at the X-ray frequencies may clarify many present uncertainties, such as the distribution of the spiral arms.

5. SCO XR-1

Several observers have derived spectral data for SCO XR-1 and have fit their measurements to thermal models. We also do this in Chapter 7. The higher energy X-ray data have been used to set a value for the assumed plasma temperature (= KT). The accuracy of the value of KT is limited by the small range and statistical accuracy of the high energy data. The lower energy data were fitted by putting in the appropriate amount of interstellar medium and calculating the absorption using the Brown and Gould (21) absorption coefficients (figure 2b).

Our measurements indicate a drop in the spectrum below 3 Kev. From the strength of the interstellar medium, it is estimated that the distance to SCO XR-1 ranges between 300 pc. and one kiloparsec (~ 600 pc).

The lifetime for free-emission from an optically thin hot plasma is proportional to the square root of the temperature and the reciprocal of the electron density. Johnson (1967) has calculated the cooling time for various values of the radius R and the electron density N_e. For $R = 10^{15}$ cm and $N_e = 3 \times 10^3 \text{cm}^{-3}$, the cooling time is about 10 years. These estimates clearly indicate the requirement for a continuous supply of energy to the radiating plasma.

In the absence of a very massive stellar core, or strong magnetic field, the pressure of the hot gas would cause the cloud to blow up. Without gravitational or magnetic confinement, the cloud would expand through 1 arc second in about 0.3 year. For $R = 10^{15}$ cm, the requirement for gravitational confinement is $5 \times 10^4 M_\odot$; for magnetic confinement H is about 1G. If $R = 10^{10}$ cm, the required mass is only $5 M_\odot$ and the magnetic field is 6×10^3 G. A neutron star could easily provide the gravitational confinement and would very likely provide the magnetic-field requirement as well.

Cameron (23) has suggested a model consisting of a vibrating neutron star with a surrounding corona or magnetosphere. The neutron star is expected to vibrate radially with a period of the order of a minute or less, and may store up to 10^{51} to 10^{52} ergs. of mechanical vibrational energy in the supernova event. A corona around the neutron star expanding into a stellar wind would draw the magnetic lines of force out radially and rotation of the star could then twist the field lines until they reconnected to form a magnetosphere. Hydromagnetic waves driven by the stellar vibrations could be a source of electron acceleration to relativistic energies with the accompaniment of synchrotron X-rays. Or the mechanical vibration may supply energy to a high-temperature corona which would produce X-ray bremsstrahlung.

The energy source is unknown, but could be related to the idea of a close binary (24) whose streaming plasma transfers are accompanied by shock collisions (25) or the like, drawing energy essentially from the gravitational and thermal store of the stars. The optical emission would on this view come from a cooler plasma volume, only partly ionized (26).

6. SPECTRAL ANALYSIS

In the variety of observations that have been made, the observing techniques are essentially similar. The basic detection system consists of a collimator that transmits incident X-rays arriving within a restricted range of angles and an X-ray detector records the number of transmitted X-rays. The gas proportional counter, because of its high efficiency and low noise, has found widest application as a soft X-ray detector. The collimator-detector problem is compounded by the requirement for large apertures. The early experiments by Giacconi, et al. (3) utilized 10 cm^2 of area. In our experiment we have used 1058 cm^2 of detector area. The expected counting rate per unit area of the detector can be expressed by the relation:

$$G(Y) = A \int_0^\infty F(E) \eta(E) e^{-N\sigma(E)} \tau(E) R(E,Y) \, dE \quad \cdots \cdots \, 12$$

counts/Kev/cm^2/sec, where

A   is a fitting factor which represents the intensity of the source.

F(E) is the assumed model function for the source.

η(E) is the measured counter efficiency.

N   is the number of hydrogen atoms/cm^2 in the line of sight.

σ(E) is the absorption cross section per hydrogen atom for the interstellar medium.

τ(E) is the transmission of the residual atmosphere in the line of sight, and

R(E,Y) is the probability of obtaining a pulse of height Y from an X-ray of energy E, and is derived from preflight resolution measurements.

The expected counting rate per channel (energy interval) and per unit

area is given by

$$G_{ij} = \int_{Y_i}^{Y_j} G(Y) \, dY \qquad \ldots \ldots \ldots \ldots \ldots 12'$$

where Y_i and Y_j are the lower and upper limit of each channel.

The counter efficiency η, the resolution function R, the atmospheric absorption τ, and the absorption cross section σ are inserted into the computer program. The input spectrum F and amount of hydrogen N are varied to produce the best fit to the data.

To obtain quantitative estimates of the observable parameters, it is customary to apply the conventional least-squares techniques in which one compares observed counting rates (G) with expected counting rates (G') according to the prescription:

$$\chi^2 = \sum_i \frac{(G_i - G_i')^2}{\delta_i^2} \qquad \ldots \ldots \ldots 13$$, i = number of channels

where δ_i is the standard deviation of the ith measurement. The values of free parameters in G' which minimize X^2 are taken to be the best value of those parameters. The minimum value of X^2 determines the goodness of fit; i.e., the probability that the expression used as G' would yield the observed data and gives an associated value for the intensity of the source (A).

We have used two free parameters. One is the number of hydrogen atoms/cm^2 in the line of sight (N) and the other is related to the kind of model used in specifying function F.

Thermal Bremsstrahlung Model:

-Simple approximation (exponential model)

$$F(E) = \frac{1}{E} \exp(-E/KT) \quad \cdots\cdots\cdots\cdots 14$$

-Free parameter = T (temperature of the source)

-More accurate approximation (with Elwert's factor)

$$F(E) = \frac{1}{E}\left[\exp(-E/2KT)\, K_0(E/2KT)\right]/\sqrt{KT} \quad \cdot\cdot 15$$

Free parameter = T (temperature of the source)

-Power Law Model

$$F(E) = E^{-\alpha_1} \quad \cdots\cdots\cdots\cdots\cdots\cdots 16$$

Free parameter: $\alpha_1 = \dfrac{K+1}{2}$ (where E^{-K} is the power law spectrum of

electrons producing the synchrotron radiation or inverse Compton effect).

-"Black Body" Model

$$F(E) = E^2/\left[\exp(E/KT) - 1\right] \quad \cdots\cdots\cdots\cdots 17$$

Free parameter = T (temperature of the source)

For the resolution function R we have used the Poisson distribution:

$$R(E,Y) = \frac{1}{Q}\exp(-E/Q)\,\frac{(E/Q)^{Y/Q}}{(Y/Q)!} \quad \cdots\cdot 18$$

Where: Y is the pulse height associated with the X-ray energy E.

Q is the "Quantum Size": change in E represented by an extra

particle counted.

$(Y/Q)! = \Gamma(1 + Y/Q),$ Γ = Gamma function

7. FIT OF SCO XR-1 MEASURED DATA TO THE DIFFERENT MODELS. DISCUSSION

7.1 Characteristics of the Experiment

We have used a freely spinning AEROBEE 150 Rocket (spin rate of 10°/sec).

-Time and Place of Launching: June 22 at 05.30 UT in Natal, Brazil.

-Altitude of SCO XR-1 Scanning: 108 Km.

-Kind of Counter Used: Proportional Counter with 1058 cm^2 of detection area and honeycomb collimator with a collimation of 12°20' full width half maximum (FWHM). It was filled with a mixed gas of argon (90%) and methane (10%) at   1 atmospheric pressure and   2.5 cm deep.

-Window Material and Thickness: 5 microns "Mylar" with a 200 $\overset{o}{A}$ "Nichrome" coating. A laboratory calibration of the window was made at 14.6 $\overset{o}{A}$ and 44.6 $\overset{o}{A}$. The detection efficiency of the counter is shown in fig. 1.

-The data from the detector were amplified and fed to a twelve-channel pulse height analyzer for the energy range from 0.1 Kev to 10 Kev. The output of each channel was telemetered to the ground.

7.2 Spectrum Analysis

The analog data was reduced using two methods. The first one was based on the "triangle" response of the counter and the second one on the "linear" response of the ratemeter (454 counts/volt) analyzed only up to saturation (2000 cps). The second method gave better X^2 results. The following table shows the measured data for both methods corresponding to each energy channel. For the interstellar absorption cross sections and efficiency of the counter, we have used values from the curves shown in fig. 2b and fig. 1, respectively. For atmospheric absorption correction we have used values from CIRA (1969) at 108 Km. Finally, for the resolution function we have measured the Quantum size Q = .0432 Kev.

In the following pages we present the obtained parameters associated with each model for SCO XR-1 with the corresponding curves. In the appendix we give the computer program discussing briefly how we have used it.

Channel	Energy Edges (Kev)	Method 1 (counts/sec)	Method 2 (counts/sec)
1	0.13-0.24	---	-
2	0.24-0.68	40	7
3	0.68-1.18	74	35
4	1.18-1.58	74	47
5	1.58-2.06	228	68
6	2.06-2.76	310	80
7	2.76-3.24	294	72
8	3.24-4.27	408	88
9	4.27-6.93	587	107
10	6.93-8.05	122	21
11	8.05-9.50	49	9
12	9.50- ∞	24	6

The data (in counts/sec) as reduced by two methods of data analysis is shown. Method 1: Triangle response; Method 2: Linear response up to saturation.

7.3 Thermal Bremsstrahlung from a Hot Plasma

7.3.1 Exponential approximation

Using equation 14 as a representation for function F(E), the number of counts per cm^2 per sec, according to 12 and 12', is:

$$G = A \int_{Y_i}^{Y_j} dY \int \eta(E) \, \zeta(E) \, e^{-N\sigma(E)} \, \frac{e^{-E/KT}}{E} \left[\frac{1}{Q} \, e^{-E/Q} \, \frac{(E/Q)^{Y/Q}}{(Y/Q)!} \right] dE$$

where the different symbols and parameters have already been defined.

The free parameters we have found for this model (associated with the minimum X^2 value) are a temperature corresponding to 7.1 Kev and a column density of absorbing atoms of 2.3 x 10^{21} atoms/cm^2.

Fig. 3 shows the measured data and the calculated curves both with and without interstellar absorption.

7.3.2 More accurate approximation with Elwert's Factor

For this approximation we have used the function F(E) expressed in equation 15. The minimum X^2 is found with a temperature corresponding to 9.8 Kev and a column density of absorbing atoms of 1.8 x 10^{21} atoms/cm^2.

Fig. 4 shows the measured data and the calculated curves for this model both with and without interstellar absorption.

7.4 Black Body Model

We have used equation 17 as a representation for function F(E). The correlated values of free parameters to the minimum X^2 (which was an order of magnitude larger than the value found for the Bremsstrahlung model) are a temperature corresponding to 6.5 Kev and an absorbing column density of 2.8 x 10^{21} atoms/cm^2.

7.5 Power Law Model

The function F(E) used in this model is represented by equation 16. We have found a minimum X^2 value for a spectral index of 4.2 and a column density of absorbing atoms of 2.2 x 10^{21} atoms/cm^2.

The relative value of the minimum X^2 for this model is even larger than that found for the Black Body model.

The best X^2 of our analysis is related to the Thermal Bremsstrahlung model with Elwert's factor. In the following table we present a relative comparison of the minimum X^2 values from the different models.

MODEL	PROCESS	X^2 relative to Model 1
1	TBHP* with Elwert's factor	1
2	TBHP* Exponential	1.4
3	Black Body	11.6
4	Power Law	17.4

TBHP*: Thermal Bremsstrahlung from a Hot Plasma

According to this result we assume that the physical process associated with X-ray emission in SCO XR-1 is Thermal Bremsstrahlung from a Hot Plasma.

The following is a calculation of the energy flux density of SCO XR-1 at 4 Kev for models 1 and 2.

Model	$(10^7 {}^\circ K)$ Temperature	Flux of 4 Kev Photons $(cm^2 \ sec \ Kev)^{-1}$
1	11.4	8.9
2	8.2	10.6

The fact that the absorbing column density we have found for the model with the best x^2 value (1.8 x 10^{21} atoms/cm^2) may signify that a possible distance to SCO XR-1 is 600 parsec if we assume a uniform interstellar medium density of 1 atom/cm^3.

8. CONCLUSIONS

According to our results the best model for SCO XR-1 is Thermal Bremsstrahlung from a Hot Plasma with a temperature corresponding to 9.8 Kev and a column density of absorbing atoms of 1.8×10^{21} atoms/cm^2. The measured energy range goes from 0.1 Kev to 10.0 Kev.

These results are in agreement with those of the Lawrence Radiation Laboratory X-Ray Astronomy Group (to be published). They searched SCO XR-1 at the same energy range one year before (spring, 1968) finding a temperature corresponding to 9.0 Kev and a column density of absorbing atoms of 1.5×10^{21} atoms/cm^2.

The observed decrease of spectral intensity with decrease in photon energy has been interpreted as absorption in cool (non-ionized) material. The absorption in excess of that in the interstellar material must be due to absorption in or around SCO XR-1 itself. The region which emits X-rays in this object is thought to be small (Chodil, et al., 1968), perhaps a hot plasma surrounding a collapsed star which is a member of a binary system.

We have also included in our analysis the other classical models, namely, Power Law and Black Body models. The fitting parameter shows that these models cannot be used for SCO XR-1.

Finally we expect that a possible distance to SCO XR-1 is 600 parsec if a uniform interstellar medium density of 1 atom/cm^3 is assumed.

9. FIGURES

Fig. 1 - Argon-Methane counter efficiency (used in the experiment). Window 5 μ Mylar. Pronounced peaks indicate the Carbon and Oxygen K-absorption edges.

Fig. 2a - Alternation of electromagnetic radiation in the atmosphere. Solid curves indicate altitude (and corresponding pressure expressed as a fraction of one atmosphere) at which a given attenuation occurs for radiation of a given wavelength. (Figure taken from reference 9.)

Fig. 2b - Total photoionization cross section per hydrogen atom as a function of incident photon energy. The elements responsible for the jumps due to their respective K-edges are indicated. The energies of these K-thresholds have been tabulated by Felten and Gould (20). (Figure taken from reference 21.)

Fig. 3 - SCO XR-1 count rate spectrum for TBHP* exponential model. Crossed marks indicate measurements and solid lines indicate the calculated response of the counter system with KT = 7.1 Kev and absorption of cosmic material with an atomic hydrogen column density of 0 atoms/cm^2 and 2.3 x 10^{21} atoms/cm^2.

Fig. 4 - SCO XR-1 count rate spectrum for TBHP* with Elwert's factor. Crossed marks indicate measurements and solid lines indicate the calculated response of the counter system with KT = 9.8 Kev and absorption of cosmic material with an atomic hydrogen column density of 0 atoms/cm^2 and 1.8 x 10^{21} atoms/cm^2.

TBHP* : Thermal Bremsstrahlung from a Hot Plasma

Fig. 1

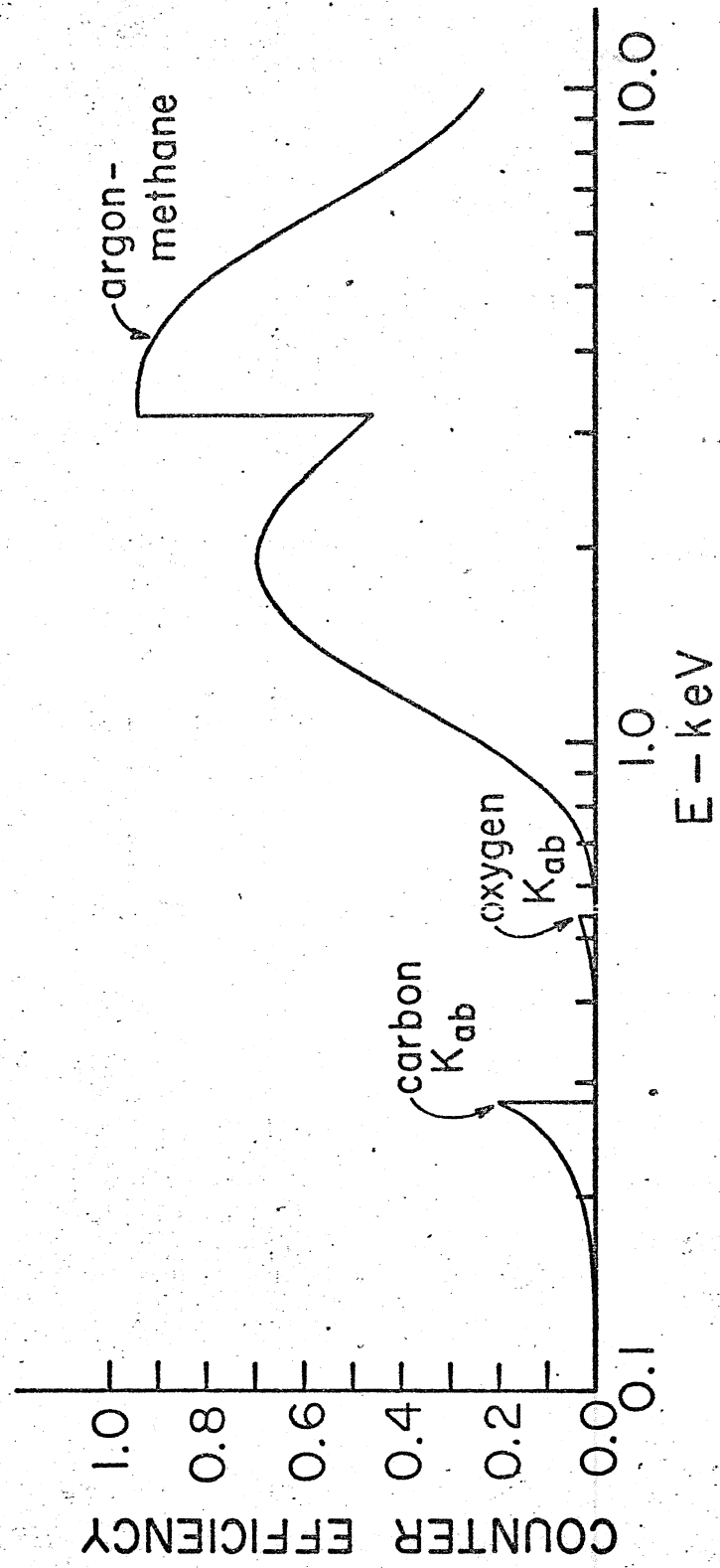Fig. 2a

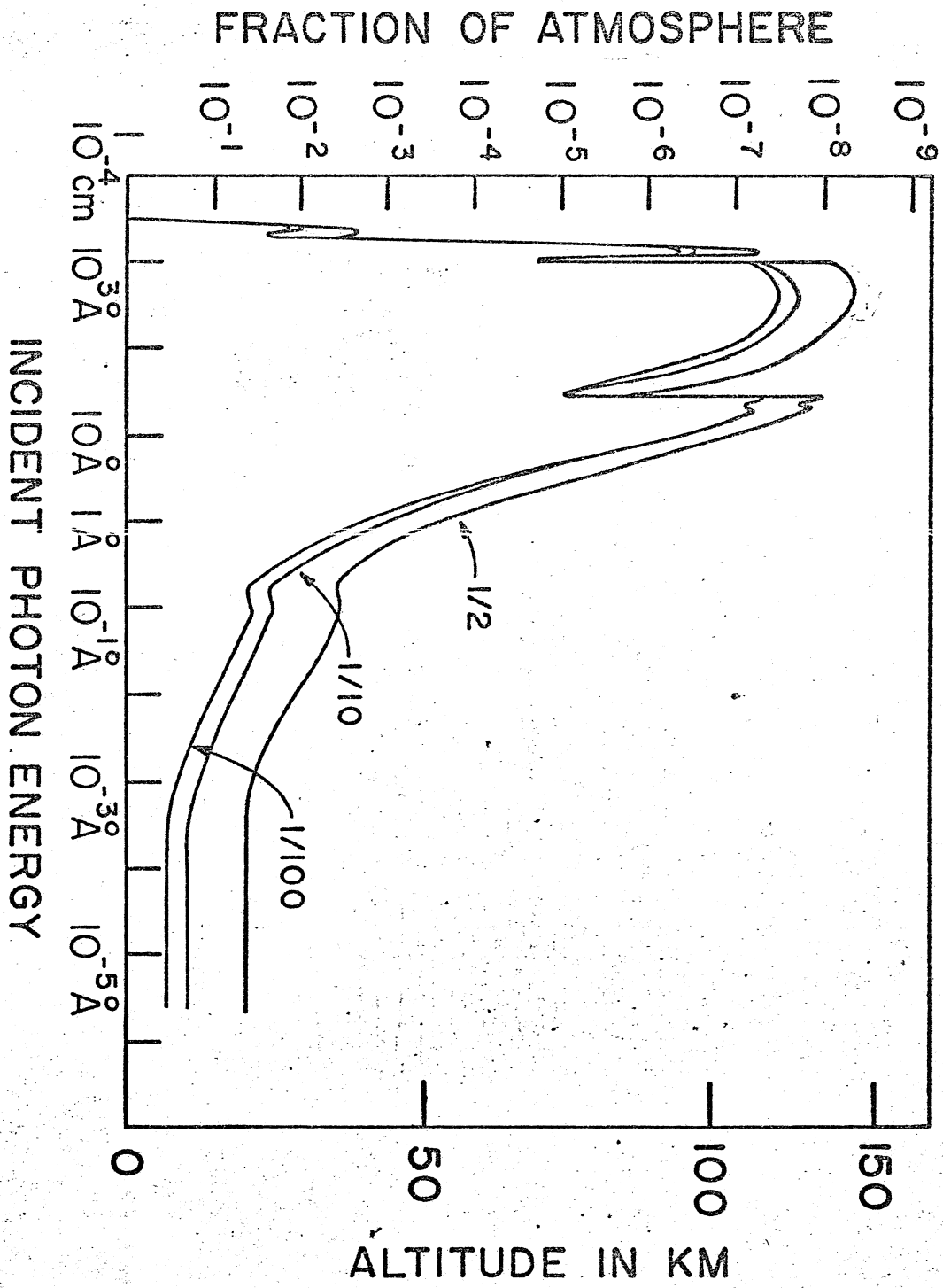FRACTION OF ATMOSPHERE

INCIDENT PHOTON ENERGY

ALTITUDE IN KM
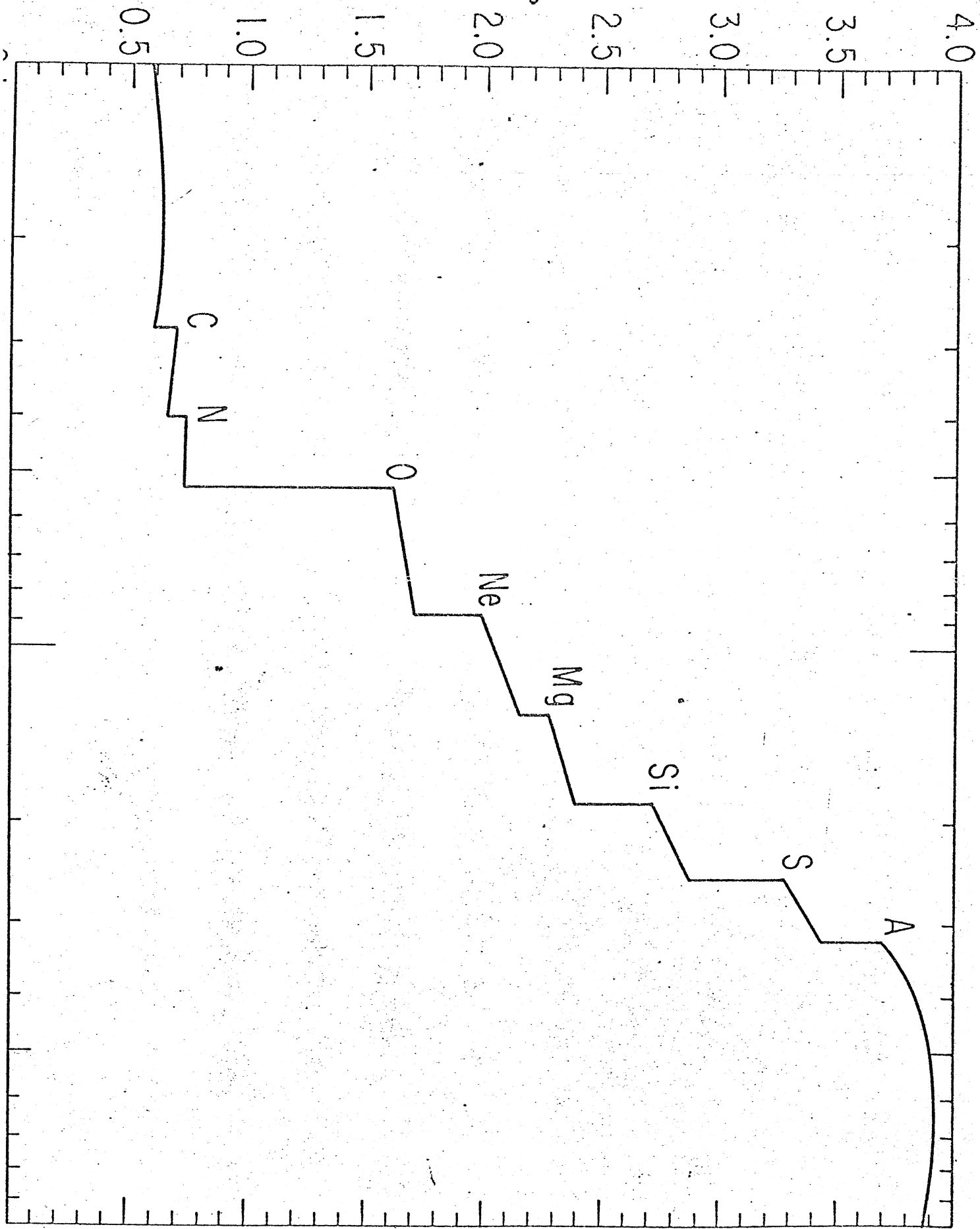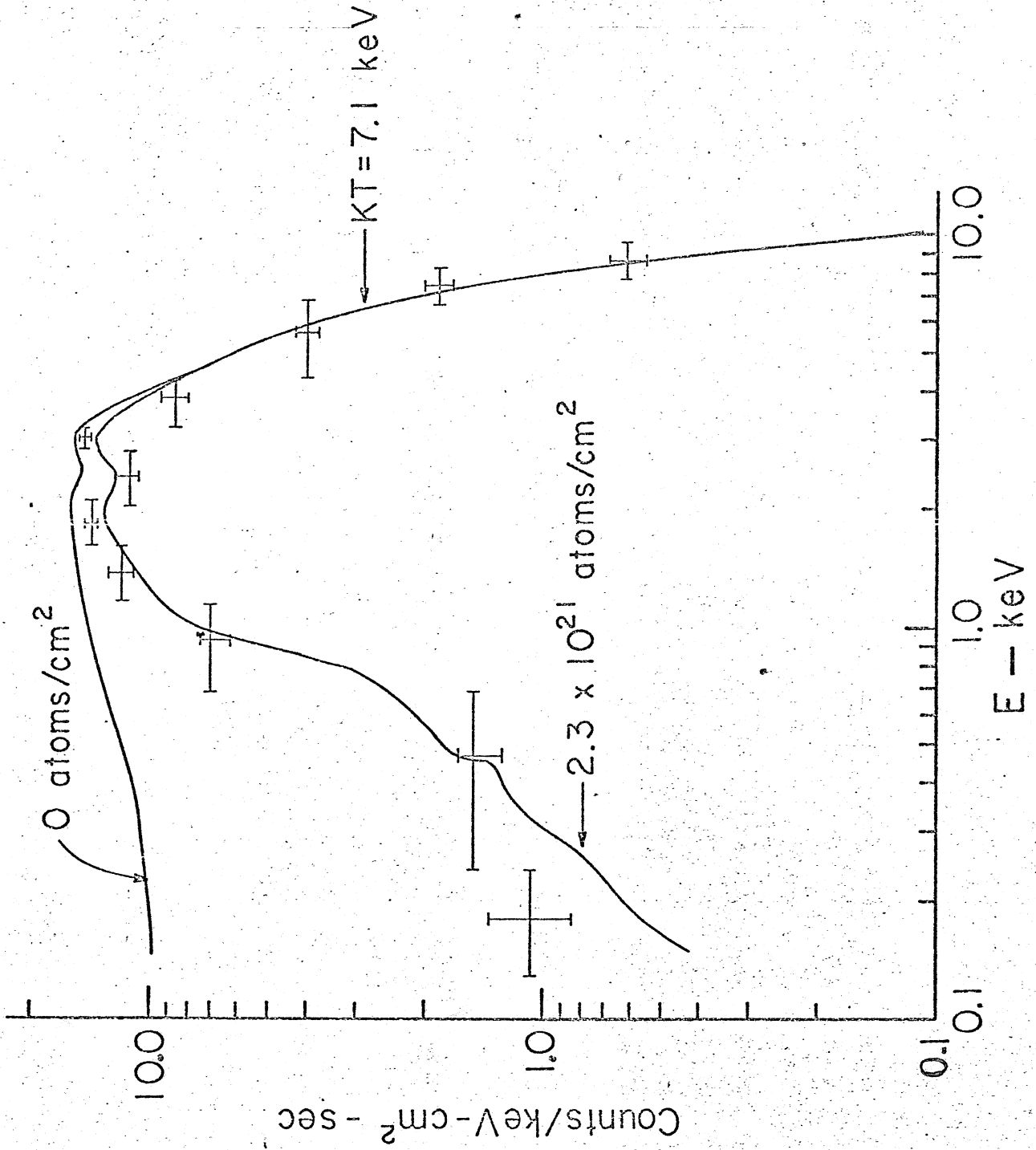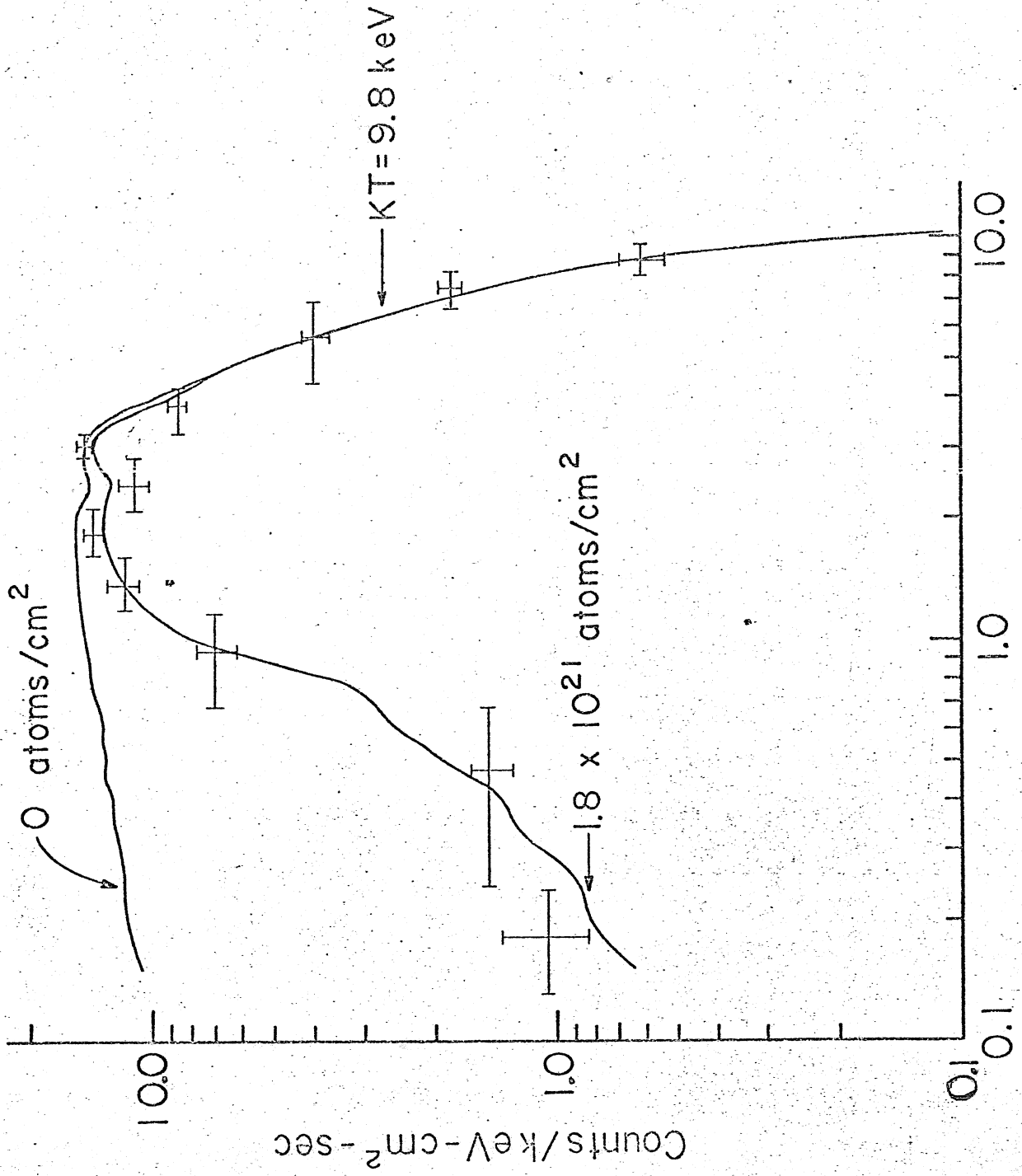
Fig. 2b

Fig. 3

Fig. 4

APPENDIX

10. DISCUSSION OF THE COMPUTER PROGRAM

The program was written in order to calculate the integral

$$G = A \int_{Y_i}^{Y_j} dY \int_0^{\infty} \eta(E)\, \tau(E)\, e^{-N\sigma(E)}\, F(E) \left[\frac{1}{Q} e^{-E/Q} \frac{(E/Q)^{Y/Q}}{(Y/Q)!} \right] dE$$

for each energy channel and to fit the measured data to those results for

the set of free parameters associated to the model specified by $F(E)$ and for

the minimum value of the x^2 test.

The Program reads tabulated values for the counter efficiency(η),

atmosphere absorption (τ), and total interstellar absorption cross section

(σ) for each value of the photon energy (E).

We insert the appropriate function $F(E)$ for each model and we calculate

the integral using Simpson rule approximation. The energy range (.1 to 10 Kev)

was split into two sets of 20 intervals (from .1 to 1 and from 1 to 10 Kevs).

The term in the denominator $(Y/Q)!$ was calculated using the Gamma function

(Γ).

$$(Y/Q)! = \Gamma\left(1 + Y/Q\right) = \int_0^{\infty} e^{-t}\, t^{Y/Q}\, dt$$

For values of $Y/Q < 50$ we used a subroutine in order to calculate the

Gamma function. For values of $Y/Q \geqslant 50$, we used the asymptotic approximation

of the Gamma function for large values of the argument

$$\Gamma(x) = x^x\, e^{-x}\, \sqrt{2\pi x}$$

. . . . , for large values of x

The program calculates x^2 values for each set of the two free parameters

of each model. Associated with that value of x^2 we have also the multipli-

cation factor of the integral A representing the intensity of the flux.

We present an example of the program for the exponential* model.

In this case we insert 4 values for the interstellar medium density $(0, 5 \times 10^{20}, 10^{21}$ and 5×10^{21} atoms/cm^2) and a range of temperatures for the source from 10^7 to 2×10^8 °K in additive steps of 10^7 °K.

With a change of a few cards we can study the different models according the function F(E) with a desired set of values for the free parameters. In the following table we identify the symbols used in the program with those defined in the main text.

PROGRAM SYMBOLS	SYMBOLS DEFINED BEFORE
G	G
Y	Y
GA	GAMMA
E	E
D	η
PSI	σ
F	Defined in the program
SIMP	Defined in the program (Simpson Rule)
GT	G(Y)
CH	Lower edge value of the channel
EXM	Measured data
SIG	Standard deviation δ
TE	Final calculation of G
AT	For atmospheric absorption
W	Y/Q
R	E/Q
S	N σ
V	E/KT
Z	Defined in the program
X	Y/Q + 1
SQ	$\sqrt{Z}$
EX	Defined in the program
AB	For atmospheric absorption
C	Defined in the program
CS	Defined in the program
A	N(interstellar medium density)

---

*For the more accurate model using the Elwert's factor we have used a subroutine in order to calculate the modified Bessel function of second Kind.

```
      PROGRAM WGONXR (INPUT,OUTPUT)
      THIS PROGRAM CALCULATES THE CONVOLUTION OF THE SPECTRAL ANALYSIS
      FOR SCOXR-1 USING THE EXPONENTIAL MODEL
      WITH INTERSTELLAR ABSORPTION AND POISSON DISTRIBUTION FOR THE
      PC RESPONSE . IT ALSO OBTAINS THE TOTAL NUMBER OF COUNTS
      PER CHANNEL FOR THE FREELY SPINNING ROCKET AEROBEE 4.183 AND
      FINALLY IT USES THE X SQUARE TEST FOR FITTING THE RESULTS TO
      THE MEASURED X RAYS DATA
      DIMENSION G(40),Y(40),GA(40),E(50),D(50),PSI(50),F(50),SIMP(2),
     1GT(15),CH(15),EXM(12),SIG(12),TE(12),AT(40)
      DATA W,R,S,V,Z,X,SQ,EX,AB,C,CS,GT,G/11*0.,15*0.,40*0./
      READ 2, (E(I),Y(I),D(I),PSI(I),AT(I),I=1,40)
 2    FORMAT (2F6.3,F7.4,F10.3,F8.3)
      READ 3, (GA(I), I=1,22)
 3    FORMAT (E18.6)
      READ 4,(CH(J), J=1,12)
 4    FORMAT (F6.2)
      READ 5, (EXM(I),I=1,11)
 5    FORMAT (F6.1)
      A=0.
11    DO 600 IS=1,20
      T=0.1E+8*IS
      B=0.86E-7
      Q=0.0432
      DO 200 I=1,37
      W=Y(I)/Q
      X=W+1.
      DO 40 K=1,37
      R=E(K)/Q
      S=A*PSI(K)
      V=E(K)/(B*T)
      AB=3.*AT(K)
      C=R+S+V+AB
      EX=EXP(C)
      IF (X.LT.50.) GO TO 39
      Z=2.*3.1416*W
      SQ=SQRT(Z)
      CS=EXP(W)
      F(K)=D(K)*(R/W)**W*CS/(SQ*EX*E(K)*Q)
      GO TO 40
39    F(K)=D(K)*R**W/(E(K)*Q*GA(I)*EX)
40    CONTINUE
      DO 100 K=1,2
      IF (K.EQ.2) GO TO 60
50    H=0.05
      L=0
      GO TO 65
60    H=0.5
      L=18
65    SUM1=0.
      DO 70 N=1,19,18
      M=N+L
70    SUM1=F(M)+SUM1
      SUM2=0.
      DO 80 N=2,18,2
```

```
      M=N+L
30 SUM2=F(M)+SUM2
      SUM3=0.
      DO 90 N=3,17,2
      M=N+L
90 SUM3=F(M)+SUM3
      SIMP(K)=H/3.*(SUM1+4.*SUM2+2.*SUM3)
00 G(I)=SIMP(K)+G(I)
00 CONTINUE
      PRINT 6,(G(I),Y(I),G(I+1),Y(I+1),G(I+2),Y(I+2),G(I+3),Y(I+3),
     6I=1,37,4)
 6 FORMAT (1H0,4(3X,E18.6,3X,F6.3))
      PRINT 1000
00 FORMAT (1H0,///////)
      DO 300 J=1,11
      I=0
      M=J+1
      AV=0.
      DO 250 N=1,37
      IF (Y(N).GT.CH(J).AND.Y(N).LT.CH(M)) GO TO 108
      GO TO 250
08 I=I+1
      AV=AV+G(N)
50 CONTINUE
      IF (I.EQ.0) GO TO 88
      GT(J)=AV/I*(CH(M)-CH(J))
      GO TO 300
88 GT(J)=0.
00 CONTINUE
      PRINT 7,(GT(J),CH(J),GT(J+1),CH(J+1),GT(J+2),CH(J+2),
     7GT(J+3),CH(J+3),J=1,11,4)
 7 FORMAT (1H0,4(3X,E18.6,3X,F6.2))
      PRINT 1000
      DIF=0.
      DO 400 M=1,11
00 SIG(M)=SORT(EXM(M))
      DO 600 N=1,15
      SUM=0.
      DO 550 J=1,11
      TE(J)=1000.*N*GT(J)
      DIF=(EXM(J)-TE(J))/SIG(J)
50 SUM=SUM+DIF*DIF
      PRINT 8, SUM,N,T
 8 FORMAT (1H0,40X,E13.6,10X,I2,10X,E9.2)
00 CONTINUE
      PRINT 1001
01 FORMAT (1H1)
      IF(A.EQ.0.) GO TO 444
      A=A+0.0005
      IF(A.GT.0.001) GO TO 2222
      GO TO 1111
44 A=0.0005
      GO TO 1111
22 A=A+0.0035
      IF(A.GT.0.005) GO TO 2211
      GO TO 1111
```

1 STOP
  END

1 STOP
  END

11. REFERENCES

1. Kupperian, J. E., Friedman, H., Proc. CSAGI Assembly, 5th, Moscow, (1958).

2. Friedman, H., Proc. Inst. Radio Engrs., 47, 272 (1959).

3. Giacconi, R., Gursky, H., Paolini, F. R., and Rossi, B. B., Phys. Rev. Letters, 9, 439 (1962).

4. Charles, M. W., Cooke, B. A., Nuclear Instruments and Methods (to be published).

5. Van Speybroekc, L. (unpublished).

6. Bowyer, C. S., Field, G. B., and Mack, J. E., Nature, 217, 32 (1968).

7. Lukirskij, A. P., Rumsh, M. A., and Smirnov, L. A., Opt. Spekroskopija, 9, 265 and 353 (1960).

8. Clark, G., Phys. Rev. Letters, 14, 91 (1965).

9. Giacconi, R., Gursky, H., and Walters, J. R., Nature, 207, 572 (1965).

10. Chubb, T. A., Friedman, H., and Kreplin, R. W., Journal of Geophysical Research, 65, 1831 (1960).

11. Price, W. J., Nuclear Radiation Detection, 2nd ed., New York: McGraw-Hill, 1964.

12. Giacconi, R., Rossi, B., Journal of Geophysical Research, 65, 773 (1960).

13. Giacconi, R., Reidy, W. P., Zehnpfenning, T., Lindsay, J. C., and Muney, W. S., Ap. J., 142, 1274 (1965).

14. Oda, M., Applied Optics, 4, 143 (1965).

15. Jackson, J. D., Classical Electrodynamics, John Wiley & Sons, Inc., 1962, 470.

16. Schwinger, J. Phys. Rev., 75, 1912 (1949).

17. Corson, D. R., Phys. Rev., 90, 748 (1953).

18. Strom, S. E., Strom, K. M., Astron. Soc. Pacific, 73, 43 (1961).

19. Bell, K. L., Kingston, A. E., Monthly Notices, Roy. Astron. Soc., 136, 241 (1967).

20. Feltern, J. E., Gould, R. J., Phys. Rev. Letters, 17, 401 (1966).

21. Gould, R. J., Brown, R. L., _Ap. J._ (to be published).

22. Grader, R. J., Hill, R. W., Seward, F. D., and Toor, A., _Science_, _152_, 1499 (1966).

23. Cameron, A. G. W., _Nature_, _205_, 787 (1965).

24. Hayakawa, S., Matsuoka, M., _Progr. Theoret. Phys. Suppl._, _30_, 204 (1964).

25. Heiles, C., _Ap. J._, _140_, 420 (1964).

26. Matsuoka, M., Oda, M., and Ogawara, Y. (submitted to _Nature_).